Single-photon probing of plasmonic waveguides

Jason Francis and Mark Tame

School of Chemistry and Physics, University of KwaZulu-Natal, Durban, South Africa

Email: markstame@gmail.com

Abstract. Plasmonics is the study of the interaction of light and conduction electrons at metal-dielectric interfaces. Here, surface plasmon polaritons (SPPs) are hybrid photon-electron excitations that can be confined to subdiffraction scales. This feature affords enhanced coupling to emitter systems (e.g. quantum dots) to SPPs, making them suitable candidates for a wide range of on-chip quantum photonic components – most notably single-photon sources. This potential use of SPPs, along with the nonlinearity provided by emitter systems, opens up quantum plasmonics as a viable route to realising quantum information processing. In this setting, the excitation of single SPPs on waveguides via single photons and the confirmation of single-photon states upon output is an important goal. In our work we experimentally probe plasmonic waveguides with single photons and measure a second-order quantum correlation function of $g^{(2)}(0) = 0.10 \pm 0.02$. A value less than 0.5 is indicative of single-excitation states.

1. Introduction

Quantum plasmonics offers an alternative to a purely photonic realisation of quantum information processing. A major advantage it offers is the subdiffraction confinement of plasmonic modes such as SPPs and localised surface plasmons (LSPs) [1]. This allows enhanced coupling of single photons to emitter systems, such as nitrogen vacancy centres and quantum dots, by reducing the large size discrepancy between the modes [2-4]. This strong coupling makes on-chip single-photon and single-SPP sources possible [5]. Additionally, it can provide nonlinearity via the photon-blockade [6], where an emitter excited by a photon of a particular frequency cannot be further excited. This process has application in the development of active switches [7], which are useful for implementing controlled quantum logic gates.

To further motivate the suitability of SPPs for quantum information applications, several demonstrations have been made suggesting that photonic entanglement and quantum information can indeed be encoded in plasmonic states. It has been shown that polarisation-entangled photon pairs maintain entanglement after conversion to and from SPPs [8]. The same has been shown for photon-number statistics of single photons used to excite single SPPs [9].

As a first step in developing the capacity to explore further the quantum properties of single SPPs and their application to quantum information processing, we follow the lead of Di Martino *et al*. We couple single photons generated via spontaneous parametric down-conversion into SPP modes on plasmonic stripe waveguides and confirm single excitation states upon output by a measurement of the second-order correlation function at zero time delay $g^{(2)}(0)$.

1.1. Photon-number Statistics

Generally $g^{(2)}$ is a function of the time-delay τ between two measurements. At a fixed position it is a measure of the joint probability of detecting a photon at time t and another at some later time τ.

Equivalently for classical fields, it is a measure of the correlation between intensities. It can be measured at the two outputs of a beamsplitter, as in the Hanbury-Brown Twiss (HBT) intensity interferometer shown in the lower part of figure 1b. Classically it is given by [10]

$$g_{BB'}^{(2)}(\tau) = \frac{\langle I_B(t + \tau) I_{B'}(t) \rangle}{\langle I_B(t + \tau) \rangle \langle I_{B'}(t) \rangle},$$ (1)

where I_B and $I_{B'}$ are the intensities measured by detectors B and B' respectively. For a 50:50 beamsplitter (1) one be written in terms of the input intensity I. Then at zero time-delay and after applying the Cauchy-Schwartz inequality, (1) becomes

$$g_{BB'}^{(2)}(0) = \frac{\langle [I(t)]^2 \rangle}{\langle I(t) \rangle^2} = g^{(2)}(0) \geq 1.$$ (2)

Thus $g^{(2)}(0)$ has a lower bound of 1 for classical light, while for photon-number states $g^{(2)}(0)$ takes the form [11]

$$g_{BB'}^{(2)}(0) = \frac{\langle \hat{n}(\hat{n} - 1) \rangle}{\langle \hat{n} \rangle^2} = 1 - \frac{1}{n},$$ (3)

where $\hat{n}$ is the photon-number operator and n is the mean photon number. In the case of single-photon states $n = 1$ and so $g^{(2)}(0) = 0$. For $n = 2$, $g^{(2)}(0) = 0.5$, and so for a single-SPP excitation we expect a value less than 0.5 and ideally close to zero.

2. Experimental Details

To experimentally probe plasmonic waveguides a compound microscope stage was used. The stage was built to allow imaging of the waveguides as well as excitation of SPPs. SPPs could be excited using an alignment laser for the classical regime. A single-photon source, however, was used to excite single-SPPs. These two critical components are discussed in what follows.

2.1. Single-Photon Source

Spontaneous parametric down-conversion (SPDC) is a nonlinear optical process by which a photon of frequency ω_p from a pump beam is converted into a correlated photon-pair at lower frequencies and at particular angles relative to the pump. One photon of the pair is called the signal with frequency ω_s while the other is called the idler with frequency ω_i. The frequencies and angles of the output photons must satisfy the conservation of energy and momentum:

$$\omega_p = \omega_s + \omega_i$$ (4)

$$\vec{k}_p = \vec{k}_s + \vec{k}_i$$ (5)

where $\vec{k}_p$, $\vec{k}_s$, $\vec{k}_i$, are the pump, signal, and idler wavevectors respectively. This results in a conical region in which correlated photons are located on opposite sides of the pump.

In the single-photon source shown in figure 1a, a 3mm thick β-BaB$_2$O$_4$ (BBO) crystal is pumped with a 200mW continuous-wave laser of wavelength 405nm. A small percentage of pump photons undergo SPDC in the BBO crystal to produce photon-pairs with a half-opening angle 3° and a central wavelength of 810nm. A narrow wavelength band of correlated photon-pairs in arms 1 and 2 as shown, are selected by (810 ± 5) nm interference filters. These photons are then coupled into single-mode (SM) fibres. The smaller numerical aperture of these fibres acts to spatially select the centre of the down-conversion mode. This results in better correlated photon-pairs. Since the down-converted photons are

produced in pairs, a photon in arm 1 can be used to herald the arrival of a photon in arm 2. This effectively post-selects true single photons.

To measure $g^{(2)}(0)$, a HBT intensity interferometer is used and is shown in figure 1b. The single-mode fibre of arm 1 is connected to a multimode (MM) fibre through which heralding photons are decoupled and focused onto a single-photon avalanche diode detector (SPAD) A. The single-mode fibre on arm 2 which is also polarisation-maintaining (PM) is similarly connected to a multimode-mode fibre. The heralded photons from this fibre is subject to the HBT interferometer such that we may measure correlations between photo-detections at SPAD detectors B and B'. The signals from each detector are sent to a counting module (CM) which then outputs the single-photon count rates at each detector and the coincidence rates between detectors to a PC. The coincidence rate is the number of detections in B and B' collectively that occur within 8 ns (the chosen coincidence window) of a detection in A.
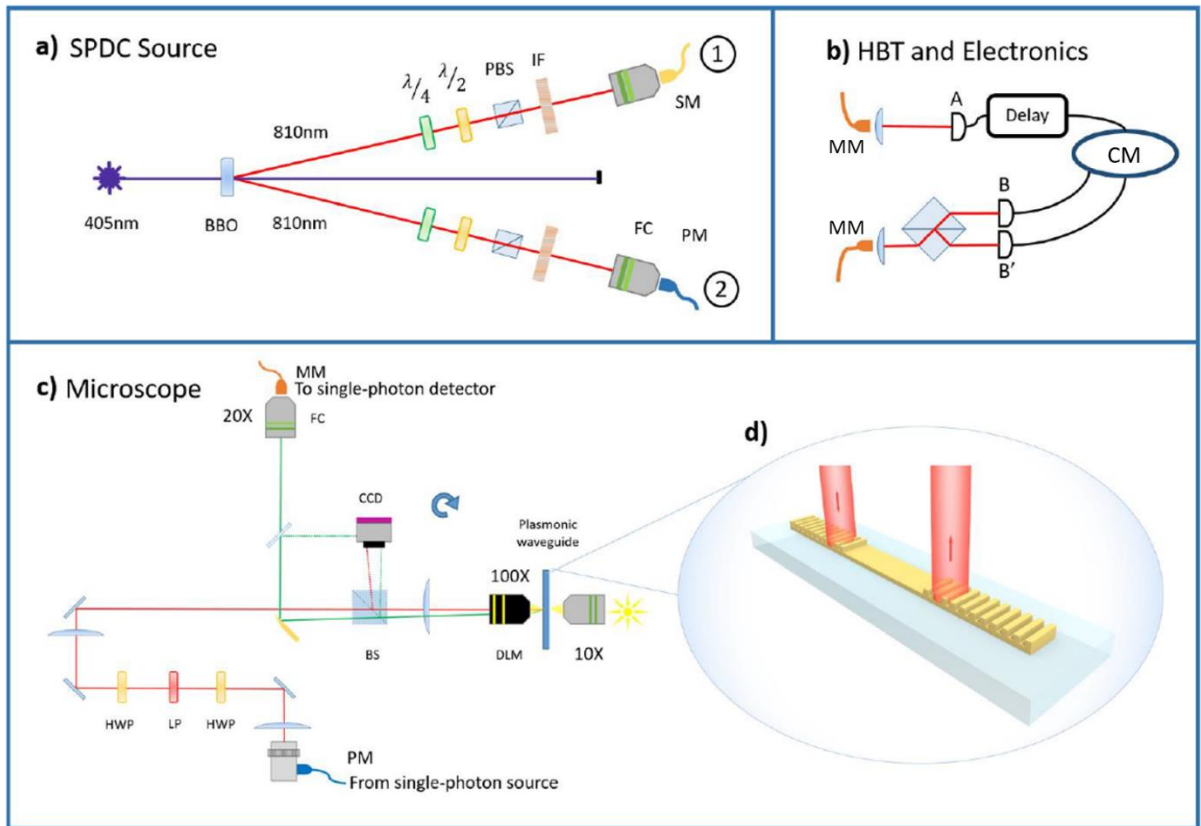

Figure 1. a) SPDC single-photon source showing all components. The waveplates are used for state tomography when the source is used to generate polarization-entangled photons. **b)** Hanbury-Brown Twiss setup with detectors and counting module needed for g$^{(2)}$ measurements. The signal from detector A is delayed to account for the length introduced by the microscope stage. The MM fibres shown are a fixture of the HBT setup, allowing it to be used with various other photon sources. The larger core of these fibres ensures a more efficient coupling to the SM fibres. **c)** Microscope used to probe the plasmonic waveguides. PM fibres were used to ensure minimal warping of the single photon polarisation and thus increase the number of photons available for SPP excitation. **d)** 3D diagram of the plasmonic waveguide supporting SPPs.

In the context of the experiment, $g^{(2)}(0)$ for single-photons can be expressed in terms of photon count rates as [9]

$$g^{(2)}(0) = \frac{N_{ABB'}N_A}{N_{AB}N_{AB'}}, \qquad (6)$$

where each factor is a count rate with a subscript indicating at which detector. Two or more subscript letters represents coincidence rates between the indicated detectors. Ideally $N_{ABB'}$ should be zero, however we find that this is not the case due to detector dark-counts, background light, and a non-zero down-conversion linewidth. The measurement procedure was to record 12 sets of all count rates with an integration time of 5s using a LABVIEW program. We then calculate $g^{(2)}(0)$ using these count rates in equation (6). Typical count rates obtained: $N_A \sim 220000\ cps$, $N_B \sim 120000\ cps$, $N_{B'} \sim 140000\ cps$, $N_{AB} \sim 4500\ cps$, $N_{AB'} \sim 5500\ cps$, $N_{ABB'} \sim 7\ cps$.

To calculate $g^{(2)}$ as a function of the delay time τ, a variable delay must be introduced on either the signal from detector B or B'. The coincidence terms in equation (6) now become functions of τ. Varying τ and collecting count rates, $g^{(2)}(\tau)$ can be calculated in the same manner as described above for $g^{(2)}(0)$. A plot of $g^{(2)}(\tau)$ will exhibit a dip at $\tau = 0$. This alone does not indicate photon sub-Poissonian statistics, which is a signature of single-photon states. Instead we require only to demonstrate that $g^{(2)}(0) < 0.5$ to confirm single excitations [11].
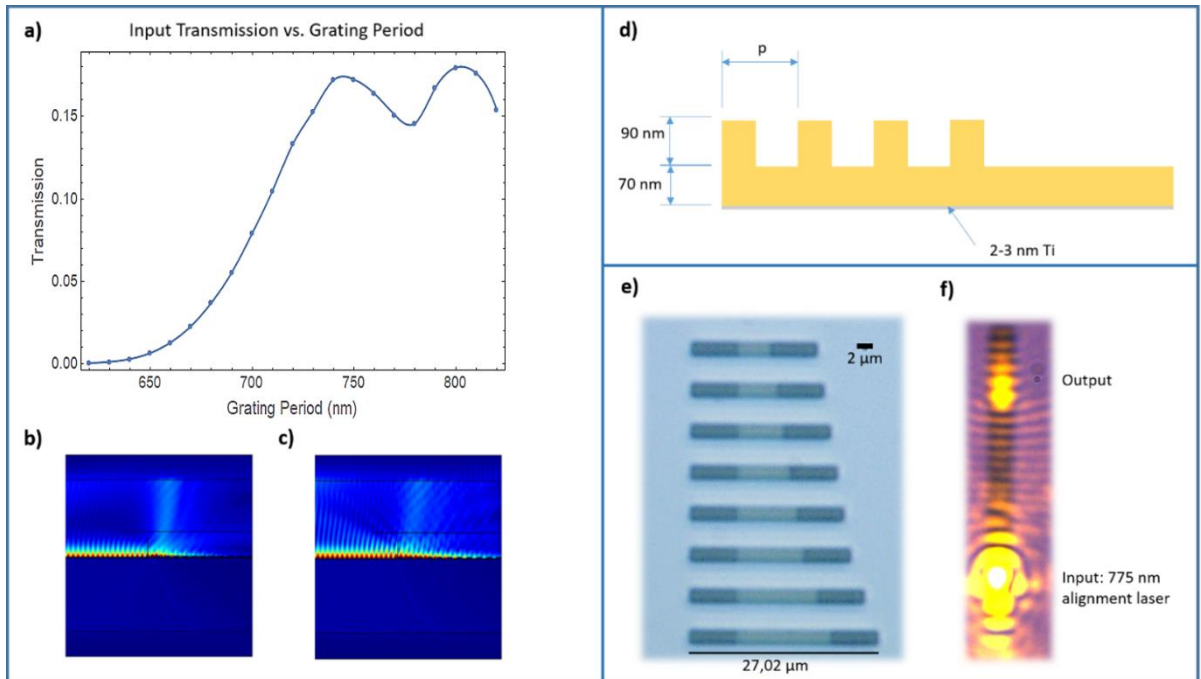

Figure 2. a) Plot of input grating efficiency as a function of the grating period. Peaks occur at 750 nm and 800 nm. **b)** Simulated electric field norm of SPP decoupled using a 740 nm grating. **c)** SPP decoupled using 800 nm grating. Note that the 740 nm period decouples the SPP more rapidly. **d)** Geometry of probed waveguides. **e), f)** Sample images obtained using the microscope setup - **f)** shows classical SPP excitation on the longest waveguide in **e)**.

2.2. Waveguide Structure and Probing Microscope

The structures probed were gold stripes $2\ \mu m$ wide and $70\ nm$ thick with a $90\ nm$ high surface-relief diffraction grating at either end. They were fabricated in a two-stage electron-beam lithography and gold evaporation process onto a silica substrate. The first stage puts the flat waveguides onto the substrate
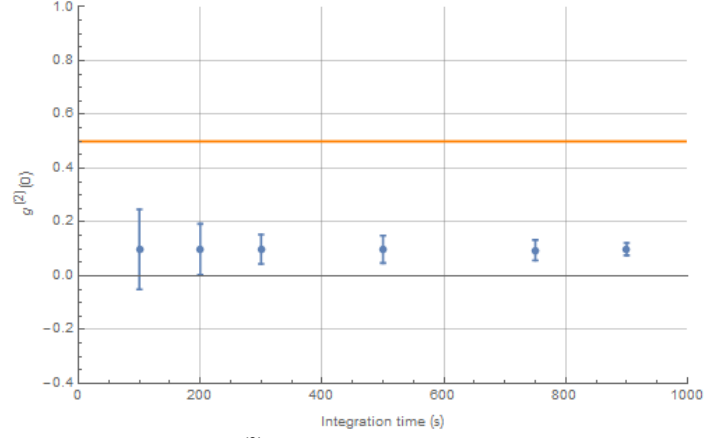
Figure 3. Single-SPP g$^{(2)}$(0) values at increasing integration times.

while the second stage applies the gratings. A range of waveguide lengths and grating periods were fabricated. To estimate the optimal period for excitation by single photons of wavelength $810\ nm$, waveguides of different periods were simulated in COMSOL to obtain their input efficiencies. The resulting graph shown in figure 2a exhibits two peaks, one at $750\ nm$ and another at $800\ nm$. The grating period chosen was $740\ nm$ (the closest to $750\ nm$ that was available). The $800\ nm$ grating proved to decouple SPPs less efficiently in the experiment.

The microscope setup used to probe the plasmonic waveguides is shown in figure 1c. The most important constituent is the diffraction-limited microscope objective which allows us to adequately image the waveguides on the CCD camera, as well as focus the input beam to a spot size of roughly $2\ \mu m$. The plasmonic chip containing a range of waveguides is mounted on a Thorlabs NanoMax XYZ translation stage to allow positioning. The input beam is injected via a PM fibre connected to a beam-collimator. To excite SPPs, the input grating of the chosen waveguide is positioned at the beam spot. Light can then be seen at the output grating when using a $775\ nm$ alignment laser. A linear polariser is used to remove any elliptical character from the input, while the first half-wave plate can be used to maximise throughput. The second half-wave plate is used to rotate the polarization such that it is parallel to the SPP propagation direction to maximise the coupling. For more efficient measurements the beamsplitter is flipped out of the beam path and a D-shaped mirror is used to pick off the output and direct it to a fibre-coupler to which a SPAD detector or spectrometer may be connected.

Once the microscope stage is aligned and optimised using the alignment laser, the PM fibre on arm 2 of the single-photon source is connected via the beam-collimator. The MM fibre leading to the HBT interferometer is then connected to the output of the microscope setup. Due to the difference in wavelength between the alignment laser and the down-conversion photons, the alignment will require adjustment. This is easiest done with higher photon rates since plasmonic waveguides suffer great loss. Higher rates are achieved by using a wider (800 ± 20) nm interference filter on arm 2. The probing system is then optimised by increasing the count rate of output photons from the waveguide. Typical count rates obtained: $N_B \sim 4000\ cps$, $N_{B\prime} \sim 4500\ cps$, $N_{AB} \sim 110\ cps$, $N_{AB\prime} \sim 120\ cps$, $N_{ABB\prime} \ll 1\ cps$.

To calculate the value of $g^{(2)}(0)$ for single-SPPs, count rates were recorded with $1\ s$ integration time for $1.5\ hours$. Due to instability over long collection times, $g^{(2)}$ was obtained for zero delay only. As mentioned in the previous section, this is sufficient for confirming single excitations are present.

3. Results

A photonic $g^{(2)}(0)$ was obtained from each of the twelve sets of count rates. The average was taken to yield a value of g$^{(2)}$(0) = 0.074 $\pm$ 0.006, which violates the classical lower bound of 1. In the SPP case, the records were grouped to obtain counts over a longer integration time. This was done to reduce error due to the low three-fold coincidence $N_{ABB\prime}$ which causes large fluctuations in the $g^{(2)}$ value. Figure 3 shows a plot of $g^{(2)}(0)$ at increasing integration times, clearly exhibiting the decrease in error.

The value at an integration time of 900 s is $g^{(2)}(0) = 0,10 \pm 0,02$. This value suggests single-excitation states upon conversion from photon to SPP.

4. Conclusion

The ability of single-SPPs to preserve the photon-number of their exciting photons has been demonstrated. A possible next step would be a more direct method to demonstrate the single-quanta nature of the excited SPPs. This can be achieved by using a plasmonic beamsplitter waveguide in place of the bulk one used in the HBT interferometer, allowing us to avoid conversion back into photons. We are now also in a position to explore coupling of SPPs to nitrogen vacancy centres for on-chip sources and switches, as well as waveguide fabrication using a newly installed atomic force microscope (AFM).

References

[1]   Maier S A 2007 *Plasmonics: Fundamentals and Applications* (Berlin: Springer)
[2]   Chang D E, Sørensen A S, Hemmer P R and Lukin M D 2006 Quantum optics with surface plasmons *Phys. Rev. Lett.* 97, 053002
[3]   Akimov A V et al. 2007 Generation of single optical plasmons in metallic nanowires coupled to quantum dots *Nature* 450, 402-406
[4]   Kolesov R et al. 2009 Wave-particle duality of single surface plasmon polaritons *Nature Phys.* 5, 470-474
[5]   Koenderink A F 2009 Plasmon nanoparticle array waveguides for single photon and single plasmon sources *Nano Lett.* 9, 4228-4233
[6]   Birnbaum K M et al. 2005 Photon blockade in an optical cavity with one trapped atom *Nature* 436, 87-90
[7]   Chang D E, Sørensen A S, Demler E A and Lukin M D 2007 A single-photon transistor using nanoscale surface plasmons *Nature Phys.* 3, 807-812
[8]   Altewischer E, van Exter M P and Woerdman J P 2002 Plasmon-assisted transmission of entangled photons Nature 418, 304306
[9]   Di Martino G et al. 2012 Quantum statistics of surface plasmon polaritons in metallic stripe waveguides *Nano Lett.* 12, 2504-2508
[10]   Thorn J J et al. 2004 Observing the quantum behaviour of light in an indergraduate laboratory *Am. J. Phys.* 72, 1210
[11]   Loudon R 2000 *The Quantum Theory of Light 3rd ed.* (Oxford: Oxford University Press)